Polymeric liquid of phosphorus at high pressure: First-principles molecular-dynamics simulations

Tetsuya Morishita*
Computational Science Division, RIKEN (The Institute of Physical and Chemical Research), 2-1 Hirosawa, Wako, Saitama, 351-0198, Japan

(Received 16 November 2001; revised manuscript received 29 January 2002; published 23 August 2002)

Constant-pressure first-principles molecular-dynamics simulations were carried out to study structural and electronic properties of the polymeric phase of liquid phosphorus at high pressures. It is found that, around 1 GPa, atoms are connected by covalent bonds by *p* electrons and accompany a Peierls distortion as in liquid arsenic. This liquid structure reflects the rhombohedral (A7) structure of crystalline phosphorus in local atomic configurations. Further compression increases the number of the first nearest neighbors and reduces the Peierls distortion. It is considered that the reduction of the Peierls distortion in the liquid phase is closely related to the transition from the A7 to simple cubic structures in crystalline phases. The characteristics of liquid phosphorus around 25 GPa and over are similar to those of liquid antimony and bismuth.

DOI: 10.1103/PhysRevB.66.054204 PACS number(s): 61.20.Ja, 61.25.−f, 71.15.Pd

I. INTRODUCTION

Solid phosphorus has several allotropes, and black phosphorus (P) is the most stable state at ambient conditions.[1] Many experiments and theoretical calculations have been performed to study its structural properties and transformations.[2–6] Black P takes the orthorhombic (A17) structure at low pressure (less than 5 GPa), but it is transformed to the rhombohedral (A7) structure around 5 GPa, and to the simple cubic (sc) structure around 10 GPa.[2] The A7 structure is regarded as a distorted sc structure. This structure is formed by an internal displacement of the fcc sublattice with a rhombohedral distortion. This is understood as a Peierls distortion[7] that stabilizes the A7 structure in a certain pressure range (5–10 GPa).[5,6] The distortion generates strong and weak atomic bonds, and this results in a coordination number N_c of 3, while N_c in the sc structure is 6. The sc structure is stably observed in a fairly wide range of pressure (10–107 GPa).[3,4] Structures with high N_c such as the bcc and simple hexagonal (sh) structures are not observed, at least, under 107 GPa.[4]

In contrast with the solid phases, liquid black P (*l*-P) has not been intensively studied so far. There was no experiment of *l*-P at high pressure until Katayama *et al.* observed the first-order liquid-liquid phase transition by pressure changes.[8] They observed drastic changes of density and the structure factor $S(Q)$ in the transition around 1 GPa. This transition was also realized in first-principles molecular dynamics (FPMD) simulations[9] with the constant-pressure technique.[10] It is clearly shown that compression causes a transformation from a molecular liquid (a low-pressure phase) to a polymeric liquid (a high-pressure phase) which is characterized by the breakup of P_4 tetrahedral molecules with large volume contraction.[9] The polymeric form is also observed in liquid arsenic (*l*-As) at ambient pressure.[11] It seems that properties of *l*-P and *l*-As are closely related, and this is of use to understand the behavior of the polymeric liquids.

In this paper, structural and electronic properties of the polymeric *l*-P at high pressures were studied by constant-pressure FPMD simulations.[12–14] Since high-pressure experiments on liquids cannot be easily performed at present, computer simulations play an important role to reveal or predict physical properties of high-pressure liquids. By means of FPMD, we can investigate liquid structures which are sensitive to changes of electronic states induced by pressure and/or temperature changes.[15–19] The constant-pressure technique[10] is desirable for simulations at various pressures. The combination of these two methods (constant-pressure FPMD) enables us to study liquid properties in a wide range of pressure.

We investigate structural changes by compression focusing on the Peierls distortion in the polymeric *l*-P. A classical description of the Peierls distortion requires the periodicity. However, it has been shown that the lattice periodicity is not necessary and that purely local considerations are sufficient for the Peierls distortion.[20] In recent experimental and theoretical studies, the survival of the Peierls distortion in liquids such as *l*-As has been confirmed.[11,15,21–25] We now show the existence of a Peierls distortion in the polymeric *l*-P, and also that it is gradually reduced by compression. Detailed studies on the behavior of the Peierls distortion according to pressure lead to a deep understanding of polymeric liquids. The relation of structural properties between *l*-P and crystalline P or liquid in group-V elements such as *l*-As will be also discussed.

This paper is organized as follows. In Sec. II, the computational method employed in this study is briefly shown. The simulation results are presented in Sec. III, and the conclusion is drawn in Sec. IV.

II. COMPUTATIONAL METHOD

The Car-Parrinello method[12] with the constant-pressure technique[10] was employed to perform constant-pressure FPMD simulations.[13,14] The simulation cell was cubic, containing 64 P atoms, and periodic boundary conditions were imposed. The norm-conserving pseudopotential[26] with "*s* nonlocality"[16] was employed to describe the electron-ion interaction. The exchange-correlation energy was described in the local density approximation (LDA) and a parametrized form by Perdew and Zunger[27] was used. Wave functions for

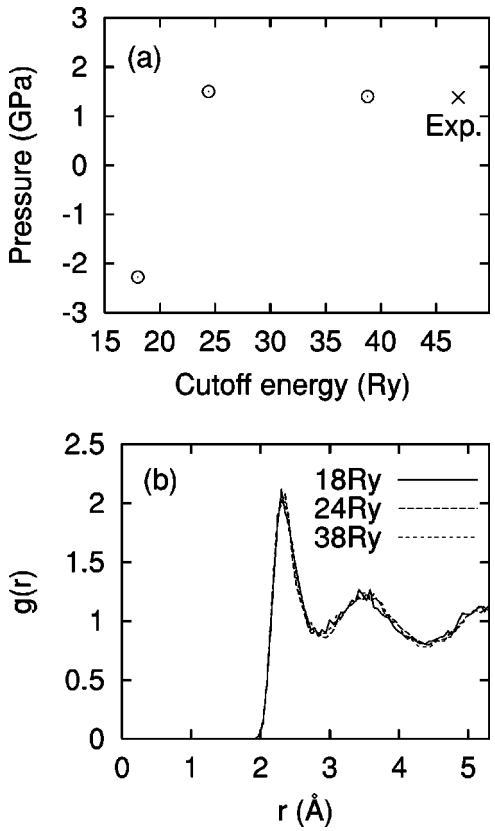

FIG. 1. (a) Dependence of pressure on cutoff energy E_{cut}. The experimental value ($\times$) is 1.38 ± 0.1 GPa (Ref. 8). (b) Pair correlation function $g(r)$ obtained in the same runs as in (a).

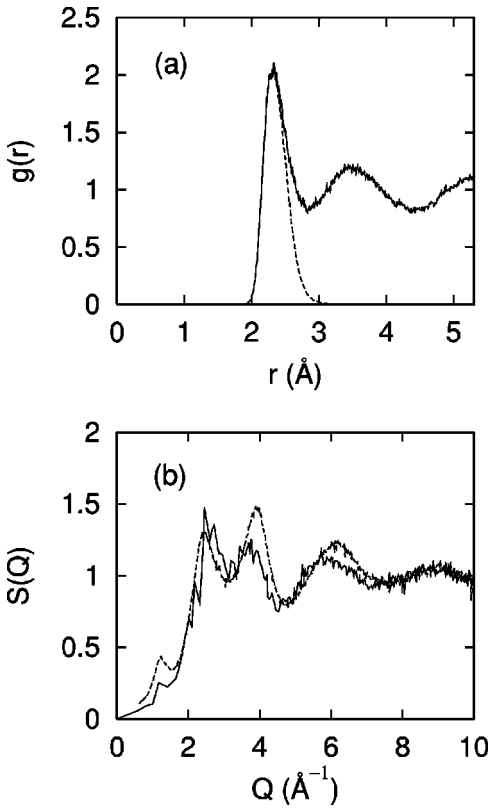

FIG. 2. (a) Pair correlation function $g(r)$ and (b) structure factor $S(Q)$ for the polymeric liquid at 1 GPa. Solid lines show the present result. Dashed lines in (a) denote the ''partial'' $g(r)$ (see the text), and those in (b) denote the experimental result (Ref. 8).

occupied valence states were expanded in a plane-wave basis with a cutoff energy E_{cut} of 24 Ry at a single point (Γ) in the Brillouin zone (BZ). It has been shown that the present conditions for the electronic state calculation are adequate to obtain accurate liquid structures.[15,16,18,28–30] Two Nosé-Hoover thermostats[31,32] connected to ionic and electronic systems, respectively, were introduced[33] to control the temperature of the ionic system, and to avoid a large deviation of the electronic states from the Born-Oppenheimer surface. Integrations of equations of motion were performed with a time step of 0.126 fs. A periodic resetting of total ionic momentum was performed to suppress the ionic flow due to thermostats.[34]

To see the dependence of the pressure values on E_{cut} in our system, we performed molecular dynamics (MD) runs of the polymeric *l*-P with E_{cut} of 18, 24, and 38 Ry, respectively under constant volume ($\rho = 2.7$ g/cm^3) at 1400 K. In Fig. 1(a), the dependence of the pressure values is shown. The corresponding experimental value (1.38 ± 0.1 GPa) (Ref. 8) is also plotted for comparison. Each pressure was obtained as a time average of the internal pressure[10,13,14] from the virial theorem. With low E_{cut} (18 Ry in this case), a negative pressure is obtained. This is consistent with previous calculations.[19,35] A low E_{cut} tends to enhance a covalent character in the atomic bonding and generate a slightly contracted volume, or a lower pressure under constant volume, especially with the LDA.[19,28] However, other properties such as static structures converge well even with a low E_{cut} that generates negative pressures. Figure 1(b) shows the pair correlation function $g(r)$ obtained in the same runs. It is confirmed that an E_{cut} of 18 Ry is sufficient for $g(r)$. Therefore, a low E_{cut} is available if we focus on only static structures in our studies. In the present case, an E_{cut} of 24 Ry is sufficient for both structural properties and the internal pressure. Thus all simulations in this paper were carried out with an E_{cut} of 24 Ry. However, we would like to remark here that the present computational conditions may not give pressures consistent with experiments in other systems. The generalized gradient approximation (GGA) for the exchange-correlation energy tends to favor a larger volume than the LDA.[36,37] This, in some cases, improves the pressure values, but in other cases, causes overcorrections:[36,38] LDA sometimes offers better properties due to the error cancellation.[38,39] Therefore, considering this large uncertainty about pressure, we should be cautious of the pressure values in FPMD as in conventional classical MD.[40]

III. RESULTS AND DISCUSSION

A. Polymeric liquid at 1 GPa

In our previous simulation,[9] we obtained the polymeric phase of *l*-P through the phase transition from the molecular liquid phase. The present simulation started with the final atomic configuration of this polymeric liquid with the computational conditions described in Sec. II. After equilibration

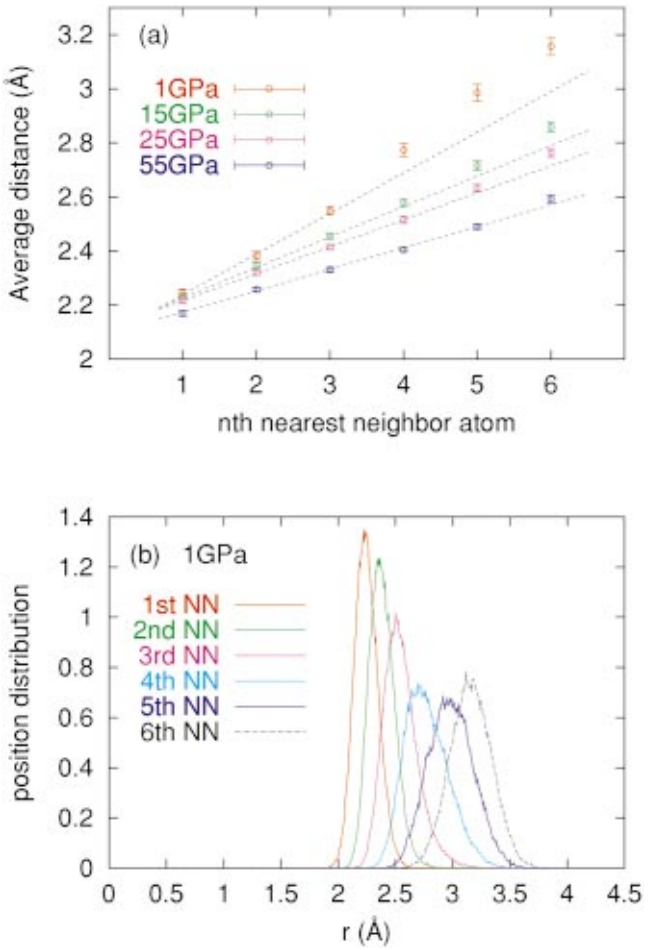

FIG. 3. (Color) (a) Average distances of the nth (1-6) NN atom at four different pressures. Short bars indicate the statistical errors and dashed lines are guides for the eyes. (b) Individual distributions of the nth (1-6) NN's positions at 1 GPa.

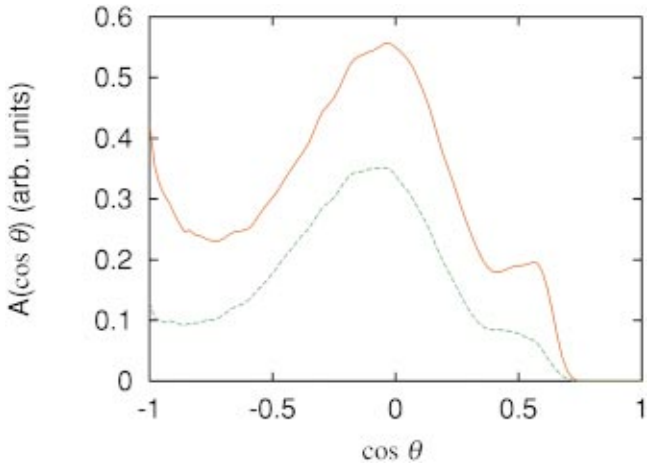

FIG. 4. (Color) Bond-angle distribution function $A(\cos\theta)$ (red lines) and the partial contribution $A_3(\cos\theta)$ from the first three NNs (green lines) at 1 GPa.

(over 5 ps), the polymeric liquid with density $\rho \sim 2.6$ g/cm^3 was obtained at 1 GPa and 1400 K. Figure 2(a) shows $g(r)$ of the polymeric liquid at 1 GPa. Also shown by dashed lines is the partial contribution from only three neighbors, i.e., the first-, second-, and third-nearest-neighbor (NN) atoms ["partial" $g(r)$].[15] The characteristic feature of this $g(r)$ is the existence of a second peak which is not found in the molecular liquid.[9] The coordination number N_c obtained by integrating $4\pi r^2 g(r)$ up to the first minimum r_m (2.79 Å) is 3.7. However, this strongly depends on the value of r_m due to the rather vague first minimum. The overall shape and N_c are consistent with those of *l*-As at ambient pressure which also has a polymeric form.[11,15,21,22] Although N_c is calculated as 3.7, the "partial" $g(r)$ containing three atoms is almost coincident with the symmetric part of the first peak of the total $g(r)$. This property is also found in *l*-As, in which characteristics of the A7 structure still remain.[15] In the A7 structure, the first nearest neighbors (NNs) of each atom are composed of three atoms connected by covalent bonds, and the second NNs are composed of three other atoms connected by long weak bonds. Taking account of these facts, the "practical" coordination number in *l*-P at 1 GPa is considered to be 3.[15] This is also supported by the average distance of the nth NN atom (n=1–6) from each atom in Fig. 3(a).[22] At 1 GPa (red circles), the first three NNs show almost linear dependence, but the three following NNs (fourth, fifth, and sixth NNs) show a different behavior. The tendency clearly changes between the third and fourth NNs. Figure 3(b) shows the individual position distributions of the nth NN atom at 1 GPa. It is easily recognized that the first three NNs have relatively high and narrow peaks, while the three following NNs have less sharp distributions. The broadened peak widths suggest the different bonding character compared with the first three NNs, which is consistent with the A7 structure. Therefore, we consider that the characteristic change between the third and fourth NNs is meaningful and that the first three NNs are connected by relatively strong (covalent) bonds in *l*-P at 1 GPa. We note that the first five NNs at 55 GPa have distributions with almost the same peak widths and heights in contrast to 1 GPa (see Sec. III B). The bond lengths of the first and second NNs in the A7 structure at 5.5 GPa are 2.20 Å and 2.81 Å, respectively.[2] These are approximately coincident with the first peak and the minimum of the $g(r)$, respectively (although the position of the first peak has slight uncertainty, see below). Also, the fourth and fifth NNs in Fig. 3(b) are mainly distributed around 2.8 Å. Therefore, it is considered that the vague first minimum is due to the contribution of the weakly bonded atoms. It should be noted that LDA tends to exaggerate the strength of such weak bonds and this is, in some cases, reflected in $g(r)$ as a vague first minimum.[17] Therefore, GGA may more clearly produce the first minimum of the $g(r)$ at 1 GPa and thus, the value of N_c. However, the above issue tends to be less important in high-density phases. Thus we believe that the present results at higher pressures are not significantly influenced by GGA.

$S(Q)$ is shown in Fig. 2(b). The overall shape is in good agreement with the experimental one. However, a slight discrepancy of the peak position is found around 6 Å^{-1}. We have confirmed that this discrepancy is related to the position

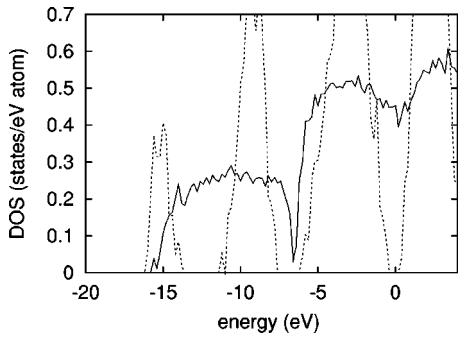

FIG. 5. Electronic density of states (DOS) for the polymeric (solid lines) and molecular (dotted lines) liquids. The Fermi energy E_F is set to 0 eV.

of the first peak of the $g(r)$ in Fig. 2(a).[15,21] In the pseudopotential electronic state calculation of P with ''*s* nonlocality,'' it is shown that the first-neighbor distance [the position of the first peak of $g(r)$] is estimated to be slightly longer than the actual one.[16] In fact, the position in the present result (2.32 Å) is slightly shifted compared with the experimental one (2.28 Å).[8] This is consistent with the previous report by Hohl and Jones.[16] We found that the modified $g(r)$ with the first peak shifted to the shorter distance can reproduce the experimental peak position around 6 Å^{-1} by Fourier transformation. Thus the origin of the discrepancy is considered to be the treatment of ''*s* nonlocality.'' The two characteristic peaks (around 2.5 and 3.7 Å^{-1}) indicate more complicated liquid structures than those of a simple liquid. They are more clearly reproduced than the previous result of *l*-As,[15] but not completely yet. This may be due to the small system size in our simulations.

The bond-angle distribution function $A(\cos\theta)$ gives more insight of the structures. It counts angles between the two vectors that join a central atom with two neighbors within a sphere of radius r_m. Figure 4 shows $A(\cos\theta)$ together with the partial contribution $A_3(\cos\theta)$ from the first three NNs. The main peak is located around $\cos\theta=-0.1$ (96°) and the subpeak is around $\cos\theta=0.5$ (60°). This shows that atoms are mainly connected by covalent (σ) bonds by *p* electrons in the polymeric phase. $A_3(\cos\theta)$ shows this more clearly. The peak position, $\cos\theta=-0.1$ (96°), is slightly deviated from $\cos\theta=0$ (90°) as in the A7 structure. This structure is regarded as a distorted sc structure by the Peierls distortion, and the bond angle within the first NNs ($N_c=3$) is ~97°. Considering that the ''practical'' coordination number is 3 in this liquid, the deviations in $A(\cos\theta)$ and $A_3(\cos\theta)$ reflect the Peierls distortion in the A7 structure.

The Peierls distortion is caused by a resolution of the degenerate states around the Fermi energy E_F into bonding and antibonding states. It has been shown that the Peierls distortion can be caused only by atomic interactions within a certain local region around each atom, not periodicity.[20] This reminds us of the Jahn-Teller distortion in molecules, which is caused by essentially the same mechanism.[41] In an isolated P atom, *p* orbitals form along three orthogonal directions. However, the generation of bonding states causes distortion (symmetry breaking) in the corresponding local geometry such as bond lengths or angles. Therefore, the deviation of

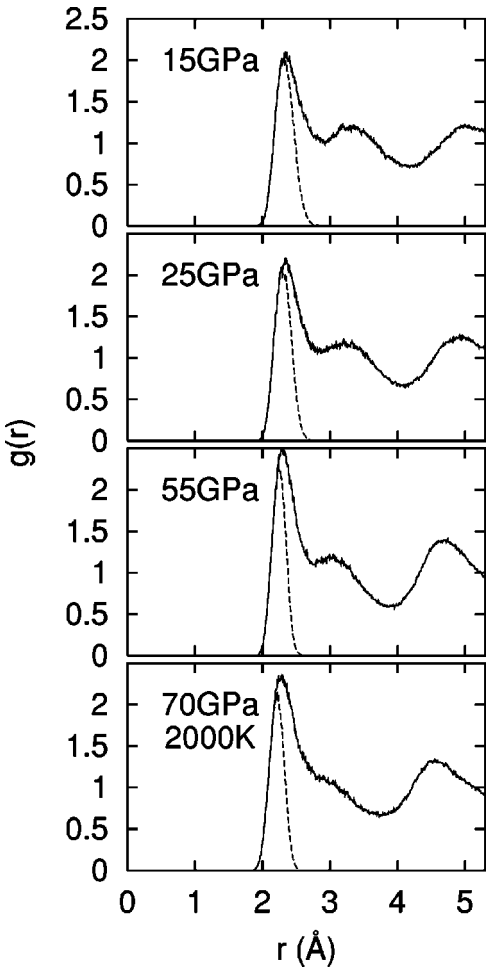

FIG. 6. $g(r)$ for *l*-P at 15, 25, 55, and 70 GPa. Dashed lines are the ''partial'' $g(r)$ as in Fig. 2.

the bond angles from 90° in this liquid can be regarded as an indication of the Peierls (or Jahn-Teller) distortion as well as N_c and bond lengths.[42] The existence of the Peierls distortion is again confirmed by the electronic density of states (DOS) below.

The subpeak in $A(\cos\theta)$ (~60°) is more clearly seen than in $A_3(\cos\theta)$. From this, we consider that the subpeak reflects the weakly bonded atoms which have relatively long bonds and favor a close-packed structure because of its isotropic interaction. This is consistent with the discussion on the vague first minimum of the $g(r)$ mentioned before.

In addition to the structural properties, the electronic DOS was also calculated. It was obtained by static electronic state calculations with 14 **k** points in the BZ for several atomic configurations in the liquid phase. These calculations were carried out by use of the CASTEP code.[43] In Fig. 5, the DOS for the polymeric phase is shown together with that for the molecular liquid phase. In the molecular phase, there are three separated bands below E_F accompanying a gap at E_F. On the other hand, the DOS in the polymeric phase has no gap around E_F showing a metalliclike character. Valence bands are clearly separated into *s* and *p* bands (the lower and upper parts, respectively). This shows that atomic bonds are

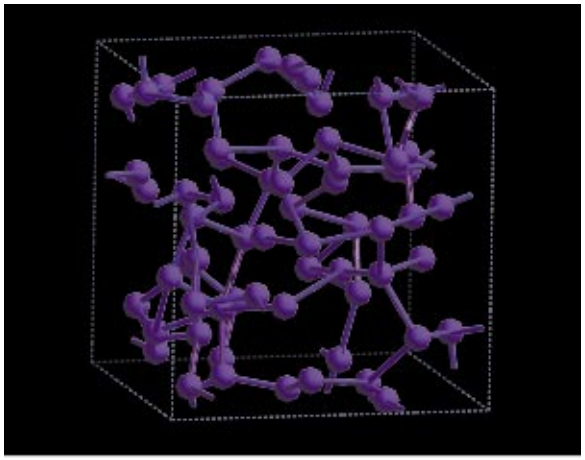

(a)

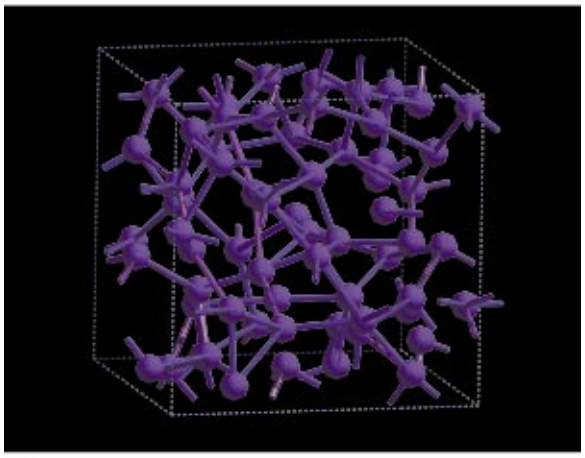

(b)

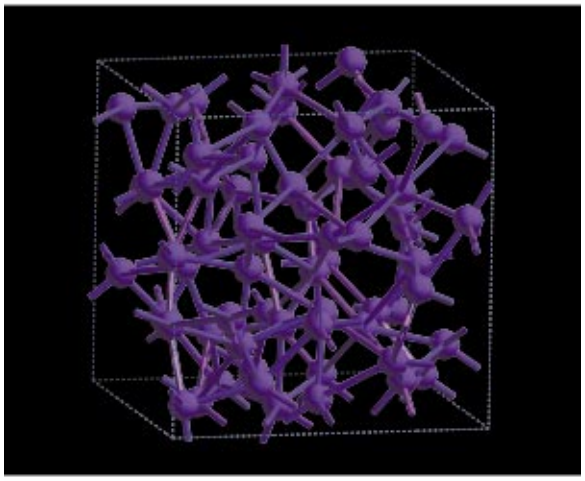

(c)

FIG. 7. (Color) Snapshots of typical atomic configurations at (a) 1, (b) 25, and (c) 55 GPa.

mainly composed of p electrons. There also exists a dip around E_F which separates the bonding and antibonding states leading to the σ bonds. This again confirms the existence of the Peierls distortion.

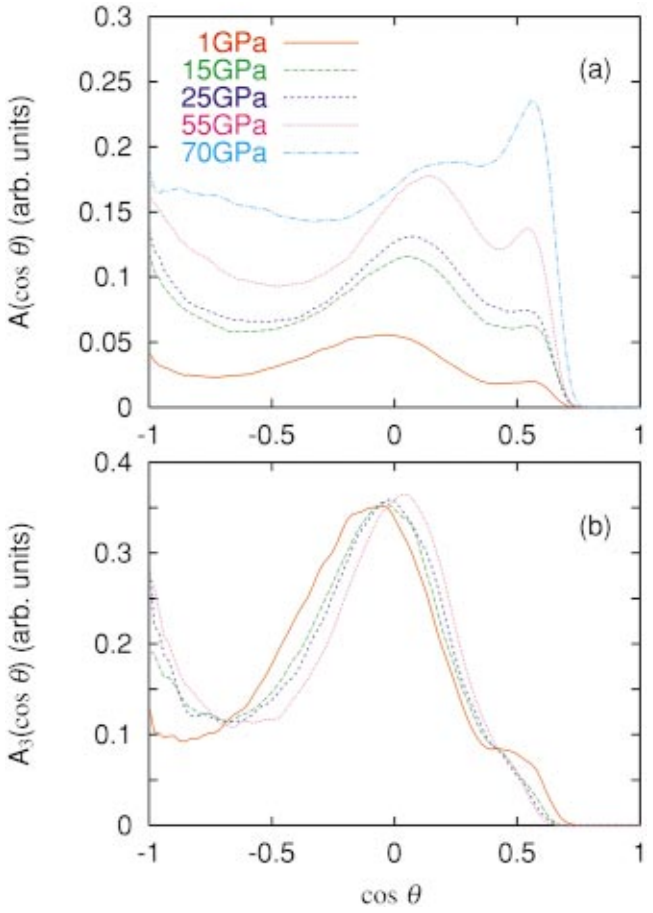

FIG. 8. (Color) (a) $A(\cos\theta)$ and (b) $A_3(\cos\theta)$ at several pressures. Only results at 1400 K are shown in (b) to show the reduction of the Peierls distortion clearly.

B. Polymeric liquid at higher pressures

Further compression on the polymeric liquid causes interesting changes of structural and electronic properties. The high-pressure liquids were obtained by compressing the polymeric liquid of 1 GPa. During the simulation with compression, the external pressure was raised by 5 GPa every 2 ps. Equilibration for 5 ps was performed at several pressures to obtain various properties. Figure 6 shows $g(r)$ at four pressures; 15, 25, and 55 GPa at 1400 K, and 70 GPa at 2000 K, respectively. At the highest pressure 70 GPa, a pressure-induced crystallization occurs at 1400 K in our simulation,[44] so that properties at 70 GPa were calculated at 2000 K where the liquid stably exists. The first peak of $g(r)$ is located around 2.3 Å at any pressure, while the second peak gradually fades away and the position of the third peak (around 5.0 Å) is shifted to the shorter distance. From the "partial" $g(r)$ for three nearest atoms (dashed lines), it is found that the number of atoms contained in the first peak is increased. N_c at each pressure is calculated as 5.5 (15 GPa), 5.9 (25 GPa), 7.0 (55 GPa), and 8.0 (70 GPa), where r_m is assumed as 2.85, 2.80, 2.75, and 2.80 Å, respectively. It is obvious that N_c is increased by compression. On the other hand, the sum of the number of atoms under the first and second peaks of

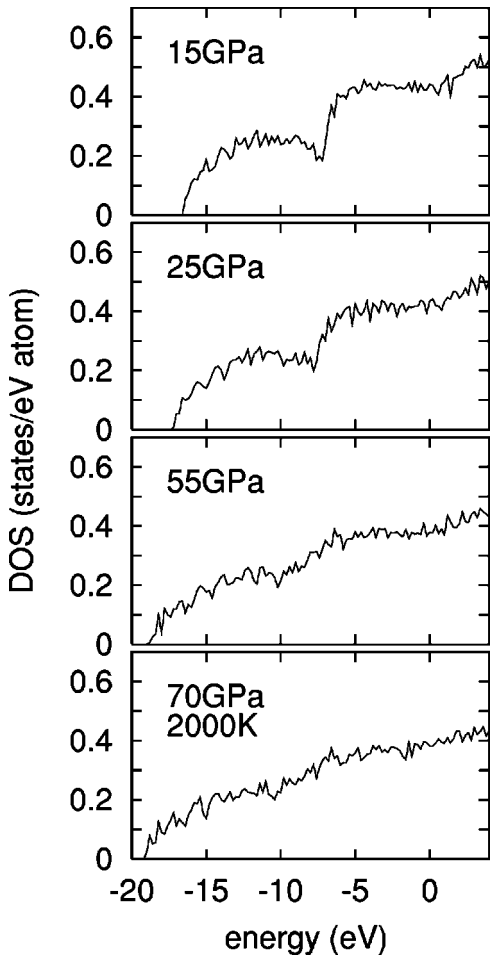

FIG. 9. DOS for *l*-P at 15, 25, 55, and 70 GPa. E_F is set to 0 eV.

$g(r)$ (integration up to ~ 4 Å) is approximately constant (~ 18) at all pressures. The overall shape of $g(r)$ at 25 GPa and over is similar to that of liquid Sb or Bi.[22–24] In *l*-Sb or Bi, N_c is much higher than 3 and the number of atoms in the first and second coordination shell is ~ 18.[22–24]

The average distance of the nth NN atom also reflects the increase of N_c [Fig. 3(a)]. The characteristic change between the third and fourth NN atoms at 1 GPa is not clearly seen at higher pressures. The difference of the atomic bonding character seems to be gradually reduced. This means the gradual incorporation of the fourth, fifth, and sixth NNs into the first coordination shell, which results in the increase of N_c.

Snapshots of typical atomic configurations at 1, 25, and 55 GPa are given in Fig. 7. The increase of N_c and the complexity of the polymeric form can be clearly confirmed.

The increase of N_c indicates the reduction of the Peierls distortion. To confirm this, we pay attention to the change of the atomic bonding character. In Fig. 8(a), $A(\cos\theta)$ at several pressures is given. It is found that the peak around $\cos\theta=0$ (90°) is gradually shifted to the smaller angle ($\cos\theta>0$), and that around $\cos\theta=0.5$ (60°) grows up by compression. This reflects the increase of atoms connected by weak bonds in the first coordination shell, which are outside of the shell at low pressures. $A_3(\cos\theta)$ at 1400 K are given in Fig. 8(b) to show the change of the atomic bonds which originally form the σ bonds at 1 GPa. This does not show considerable changes by compression compared with $A(\cos\theta)$. However, a subtle but important change is found. The peak location is slightly deviated from $\cos\theta=0$ (90°) at low pressures as described in Sec. III A, but this deviation is gradually reduced. This seems to be essentially the same phenomenon as found in the structural transformation from the A7 to sc structures: the reduction of the Peierls distortion. It has been shown that the transition from the A7 to sc structures is due to the increase of the mixing of *d* orbitals into the states around E_F.[6] This decreases the separation of the bonding and antibonding states at E_F, and weakens the σ bonds by *p* electrons, leading to a less distorted sc structure. Since the characteristics of the crystalline structures are well preserved in the liquid, we consider that the same mechanism works in the polymeric liquid. In fact, the calculated DOS at high pressures shows a consistent behavior with this mechanism (see below). Therefore, we conclude that the Peierls distortion in the liquid is reduced by compression. It should be remarked that a continuous transition from A7 to sc structures is observed at high temperature (973 K, below the melting temperature), while a discontinuous transition is observed at room temperature in experiment.[45]

It is also interesting that, even at high pressures, the peak around 90° is clearly found in $A_3(\cos\theta)$, although the peak around 60° is considerably enhanced in $A(\cos\theta)$. This indicates that there are two characteristic atomic configurations, short- and long-range orders,[9,28,29] within the first coordination shell. The persistence of a sc-like structure (the short-range order) is consistent with the strong stability of the sc structure in crystalline P. Atomic interactions in the long-range order are rather isotropic, and close to those in a simple liquid. It is expected that, at extremely high pressure, the sc-like structure almost fades away, and an isotropic interaction becomes more dominant by taking account of the structural transformations to more close-packed structures in crystals over 140 GPa (sc $\rightarrow$ sh $\rightarrow$ bcc).[3,4]

The mentioned characteristics of $A(\cos\theta)$ at high pressures are also found in *l*-Sb and Bi.[23,24] The peak around 60° is dominant in liquids of the heavy elements. It is reported that *l*-Sb has a quite weak Peierls distortion,[24] while *l*-Bi dose not contain such distortions.[23] These are consistent with *l*-P at high pressures. The similarity of the structural properties of high pressure *l*-P to those of *l*-Sb or Bi at ambient pressure is the same trend as observed in the crystalline phases.

The reduction of the Peierls distortion is also confirmed by the DOS at high pressures in Fig. 9. As the pressure is increased, the split of the valence bands found at 1 GPa (Fig. 5) is reduced, and the overall shape becomes close to that of a free-electron metal, or the sc or sh structures in crystalline P.[6,46] It is found that the small dip around E_F at 1 GPa is filled at high pressures. This means the reduction of the σ bonds by *p* electrons and consequently, of the Peierls distortion. We note that these characteristic changes in the DOS are also similar to those in the crystalline phases (A7 $\rightarrow$ sc $\rightarrow$ sh).

IV. CONCLUSION

Constant-pressure FPMD was applied to the polymeric *l*-P to investigate its structural and electronic properties at high pressures. It is shown that, around 1 GPa, atoms are connected by covalent bonds by *p* orbitals, and accompany a Peierls distortion as in *l*-As. However, in compression, structural and electronic properties gradually change and the Peierls distortion is reduced. In the compressed liquid, the split of bonding and antibonding states at E_F is reduced, and the σ bonds by *p* electrons are weakened as in *l*-Sb or Bi. Consequently, *l*-P at high pressures ($\geqslant 25$ GPa) shows a behavior similar to that in liquids of heavy elements such as Sb or Bi at ambient pressure. We note that this tendency is rarely reported in contrast with in crystalline phases. The reduction of the Peierls distortion in the polymeric liquid is considered to be closely related to the transition from the A7 to sc structures. Further compression enhances the characteristics of a simple liquidlike structure (~ 70 GPa). The second peak of $g(r)$ almost vanishes, and N_c is significantly increased. However, there is still a sc-like configuration as the short-range order within the first coordination shell. This is consistent with the strong stability of the sc crystalline phase in a wide range of pressure.[3,4] Our results suggest that much higher pressure (>70 GPa) generates more isotropic atomic interactions, and leads to a more simple liquidlike structure.

ACKNOWLEDGMENTS

The author is grateful to Dr. T. Iitaka, Dr. Y. Katayama, and Professor S. Nosé for valuable discussions, and to Professor D. M. Bird and Dr. T. Ebisuzaki for the use of the CASTEP code. The computations were carried out at Computer Center of RIKEN (The Institute of Physical and Chemical Research).

*Electronic address: tetsuya@atlas.riken.go.jp

[1] J. Donohue, *The Structures of the Elements* (Wiley, New York, 1974).
[2] T. Kikegawa and H. Iwasaki, Acta Crystallogr., Sect. B: Struct. Sci. **39**, 158 (1983).
[3] Y. Akahama, M. Kobayashi, and H. Kawamura, Phys. Rev. B **59**, 8520 (1999).
[4] Y. Akahama, H. Kawamura, S. Carlson, T.L. Bihan, and D. Häusermann, Phys. Rev. B **61**, 3139 (2000).
[5] K.J. Chang and M.L. Cohen, Phys. Rev. B **33**, 6177 (1986).
[6] T. Sasaki, K. Shindo, K. Niizeki, and A. Morita, J. Phys. Soc. Jpn. **57**, 978 (1988).
[7] R. Peierls, *Quantum Theory of Solids* (Pergamon, Oxford, 1955).
[8] Y. Katayama, T. Mizutani, W. Utsumi, O. Shimomura, M. Yamakata, and K. Funakoshi, Nature (London) **403**, 170 (2000).
[9] T. Morishita, Phys. Rev. Lett. **87**, 105701 (2001).
[10] H.C. Andersen, J. Chem. Phys. **72**, 2384 (1980).
[11] R. Bellissent, C. Bergman, R. Ceolin, and J.P. Gaspard, Phys. Rev. Lett. **59**, 661 (1987).
[12] R. Car and M. Parrinello, Phys. Rev. Lett. **55**, 2471 (1985).
[13] P. Focher *et al.*, Europhys. Lett. **26**, 345 (1994); S. Scandolo *et al.*, Phys. Rev. Lett. **74**, 4015 (1995); M. Bernasconi *et al.*, *ibid.* **76**, 2081 (1996).
[14] T. Morishita and S. Nosé, Suppl. Prog. Theor. Phys. **138**, 251 (2000); Mol. Simul. **28**, 249 (2002).
[15] X.-P. Li, Phys. Rev. B **41**, 8392 (1990).
[16] D. Hohl and R.O. Jones, Phys. Rev. B **50**, 17047 (1994).
[17] F. Kirchhoff, M.J. Gillan, J.M. Holender, G. Kresse, and J. Hafner, J. Phys.: Condens. Matter **8**, 9353 (1996).
[18] J.S. Tse and D.D. Klug, Phys. Rev. B **59**, 34 (1999).
[19] R. Stadler and M.J. Gillan, J. Phys.: Condens. Matter **12**, 6053 (2000).
[20] J.P. Gaspard, F. Marinelli, and A. Pellegatti, Europhys. Lett. **3**, 1095 (1987).
[21] J. Hafner, Phys. Rev. Lett. **62**, 784 (1989).
[22] C. Bichara, A. Pellegatti, and J.P. Gaspard, Phys. Rev. B **47**, 5002 (1993).
[23] J. Hafner and W. Jank, Phys. Rev. B **45**, 2739 (1992).
[24] K. Seifert, J. Hafner, and G. Kresse, J. Non-Cryst. Solids **205-207**, 871 (1996).
[25] J.Y. Raty, J.P. Gaspard, R. Céolin, and R. Bellissent, J. Non-Cryst. Solids **232-234**, 59 (1998).
[26] G.B. Bachelet, D.R. Hamann, and M. Schlüter, Phys. Rev. B **26**, 4199 (1982).
[27] J.P. Perdew and A. Zunger, Phys. Rev. B **23**, 5048 (1981).
[28] I. Štich, R. Car, and M. Parrinello, Phys. Rev. B **44**, 4262 (1991).
[29] V. Godlevsky, J.R. Chelikowsky, and N. Troullier, Phys. Rev. B **52**, 13281 (1995).
[30] N. Takeuchi and I.L. Garzón, Phys. Rev. B **50**, 8342 (1994).
[31] S. Nosé, Mol. Phys. **52**, 255 (1984); J. Chem. Phys. **81**, 511 (1984).
[32] W.G. Hoover, Phys. Rev. A **31**, 1695 (1985).
[33] P.E. Blöchl and M. Parrinello, Phys. Rev. B **45**, 9413 (1992).
[34] T. Morishita and S. Nosé, Phys. Rev. B **59**, 15126 (1999).
[35] P.G. Dacosta, O.H. Nielsen, and K. Kunc, J. Phys. C **19**, 3163 (1986).
[36] K. Seifert, J. Hafner, J. Furthmüller, and G. Kresse, J. Phys.: Condens. Matter **7**, 3683 (1995).
[37] G. Kresse, J. Furthmüller, and J. Hafner, Phys. Rev. B **50**, 13181 (1994).
[38] A.R. Oganov, J.P. Brodholt, and G.D. Price, Earth Planet. Sci. Lett. **184**, 555 (2001).
[39] B.B. Karki, L. Stixrude, S.J. Clark, M.C. Warren, G.J. Ackland, and J. Crain, Am. Mineral. **82**, 635 (1997).
[40] For example, A.B. Belonoshko, G. Gutierrez, R. Ahuja, and B. Johansson, Phys. Rev. B **64**, 184103 (2001).
[41] R. Hoffmann, *Solids and Surfaces* (VCH, New York, 1988).
[42] In this report, we use the term ''Peierls distortion'' rather than ''Jahn-Teller distortion'' to emphasize the close relation of *l*-P to the A7 structure: it is natural to extend the concept of the Peierls distortion to the liquid phase in which characteristics of the crystalline structure are well preserved (e. g., Refs. 11,15, and 21–25).
[43] M.C. Payne, M.P. Teter, D.C. Allan, T.A. Arias, and J.D. Joannopoulos, Rev. Mod. Phys. **64**, 1045 (1992).
[44] T. Morishita (unpublished).
[45] T. Kikegawa *et al.*, J. Appl. Crystallogr. **20**, 406 (1987).
[46] A. Nishikawa, K. Niizeki, and K. Shindo, Phys. Status Solidi B **223**, 189 (2001).